A Sub-sample Based Hybrid DWT-DCT Algorithm for Medical Imaging Applications

Suchitra Shrestha, *Student Member IEEE,* and Khan A. Wahid, *Member, IEEE*

***Abstract*—Digital image and video in their raw form require an enormous amount of storage capacity. Considering the important role played by digital imaging and video in medical and health science, it is necessary to develop a system that produces high degree of compression while preserving critical image/video information. In this paper, we propose a sub-sample based hybrid DWT-DCT algorithm that performs the discrete cosine transform on the discrete wavelet transform coefficient. Simulations have been conducted on several medical and endoscopic images, and endoscopic videos. The results show that the proposed hybrid DWT-DCT algorithm performs much better than the standalone DWT, JPEG-based DCT, and Walsh-Hadamard transform algorithms in terms of peak signal to noise ratio and visual quality with a higher compression ratio. The new scheme reduces "false contouring" and "blocking artifacts" significantly. The rate distortion analysis shows that for a fixed level of distortion, the number of bits required to transmit the hybrid coefficients would be less than those required for other schemes.**

***Index Terms*—hybrid transform, cosine transform, wavelet transform, compression ratio, image compression**

I. Introduction

DATA compression is one of the major areas of the research in image and video processing applications. With the development of computer and network technology, more multimedia-based information has been transmitted over the internet and wireless network. The data to be transmitted and stored requires unnecessary space; as a result, it is desirable to represent the information in the data with considerably fewer bits. At a same time, it must be able to reconstruct the data very close to original data. This can be achieved via an effective and efficient compression and decompression algorithm.

The Joint Photographic Expert Group (JPEG) was developed in 1992, based on the Discrete Cosine Transform (DCT). It has been one of the most widely used compression methods [1][2]. Although hardware implementation for the JPEG using the DCT is simple, the noticeable "blocking artifacts" across the block boundaries cannot be neglected at higher compression ratio. In addition, the quality of the reconstructed images is degraded by the "false contouring" effect for specific images having gradually shaded areas [3]. The main cause of false contouring effect is heavy quantization of the transform coefficients and looks like a contour map. The Discrete Wavelet Transform (DWT) based coding, on the other hand, has been emerged as another efficient tool for image compression [4-6] mainly due to its ability to display image at different resolutions and achieve higher compression ratio. The Forward Walsh Hadamard Transform (FWHT) is another option for the image and video compression applications which requires less computation as compared to DCT and DWT algorithm.

In order to benefit from the respective strengths of individual popular coding schemes, a new scheme, known as hybrid-algorithm, has been developed where two transforms techniques are implemented together. There have been few efforts devoted to such hybrid implementation. In [14], the authors have presented a hybrid transformation scheme for video coding, which minimizes prediction error. The DWT is used for intra-coding and the DCT for inter-coding. Usama presents a scalable hybrid scheme for image coding that combines both the Wavelet and the Fourier transforms [15]. An extended version of the object-based coding algorithm is presented in [16]. Yu and Mitra in [17] have introduced another form of hybrid transformation coding technique. In [18], Singh et al. have applied similar hybrid algorithm to medical images that uses 5-level DWT decomposition. Because of higher level (5 levels DWT), the scheme requires large computational resources and is not suitable for use in modern coding standards. The authors in [19] present a scalable algorithm for video coding where the DWT is performed on the DCT coefficients. The work in [20] presents a hybrid architecture where three popular transforms (i.e., Discrete Fourier transform (DFT), Discrete Cosine Transform (DCT), and the Haar Transform) have been implemented on a single chip. The work in [21] presents similar but a more efficient hybrid scheme where the three same transforms have been implemented using the structural similarity and resource sharing.

Moreover, the Fourier-Wavelet Transform can be used to

Manuscript received November 19, 2010. The work was supported by the Natural Science and Engineering Research Council of Canada (NSERC).

The authors are the Department of Electrical and Computer Engineering, University of Saskatchewan, Saskatoon, Saskatchewan, Canada. (e-mail: sus572@mail.usask.ca, khan.wahid@usask.ca).

improve the de-noising performance for images [22]; a Cosine-Wavelet hybrid structure can be used to enhance the security in digital watermarking [23], etc. There have been some reports on multiple IDCT implementations to support multiple standards [24-26], that result in improved performance.

In this paper, we present a new hybrid algorithm: the 2-level 2-D DWT followed by the 8-point 2-D DCT. The DCT is applied to the DWT low-frequency components that generally have zero mean and small variance, and accordingly results in much higher compression ratio (CR) with important information. The JPEG quantization and scaling parameters have been used [2]. In order to demonstrate the advantage of the proposed hybrid scheme, several medical images, benchmark images, and endoscopic videos have been studied. The results are compared with standalone JPEG-based DCT, DWT, and WHT schemes. The results show noticeable performance improvement with no false contouring and a higher compression ratio compared to the other stand alone schemes. The initial version of the algorithm was presented in [13]; however, the work was limited to a lower block size (i.e., 16×16) and medical images only. In this work, we generalize the algorithm and show the performance study for a block size of 32×32. It can also be extended for other image/frame resolutions. The hybrid scheme may also be suitable for medical imaging application such as, capsule endoscopic [27].

II. Discrete Cosine Transform (DCT)

The DCT for an N×N input sequence can be defined as follows [1]:

$$D_{DCT}(i,j)=\frac{1}{\sqrt{2N}}B(i)B(j)\sum_{x=0}^{N-1}\sum_{y=0}^{N-1}M(x,y) .\cos\left[\frac{(2x+1)}{2N}i\pi\right]\cos\left[\frac{(2y+1)}{2N}j\pi\right] \quad (1)$$

where,

$B(u)=\begin{cases}\frac{1}{\sqrt{2}} & if\ \ u=0\\ 1 & if\ \ u>0\end{cases}$, $M(x,y)$ is the original data of size $x\times y$.

The input image is first divided into 8×8 blocks; then the 8-point 2-D DCT is performed. The DCT coefficients are then quantized using an 8×8 quantization table [28], as described in the JPEG standard. The quantization is achieved by dividing each elements of the transformed original data matrix by corresponding element in the quantization matrix Q and rounding to the nearest integer value as shown in Eq. (2):

$$D_{quant}(i,j)=round\left(\frac{D_{DCT}(i,j)}{Q(i,j)}\right) \quad (2)$$

Further compression is achieved by applying appropriate scaling factor. In order to reconstruct the data, the rescaling and the de-quantization is performed. The de-quantized matrix is then transformed back using the inverse-DCT. The entire procedure is shown in Fig. 1.

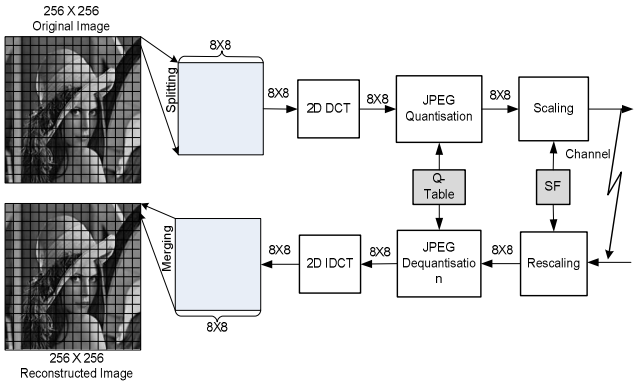

Fig. 1. Block diagram of the JPEG-based DCT scheme

III. Discrete Wavelet Transform (DWT)

The DWT represents an image as a sum of wavelet functions, known as wavelets, with different location and scale [6]. The DWT represents the image data into a set of high pass (detail) and low pass (approximate) coefficients. The image is first divided into blocks of 32×32. Each block is then passed through the two filters: the first level decomposition is performed to decompose the input data into an approximation and detail coefficients. After obtaining the transformed matrix, the detail and approximate coefficients are separated as LL, HL, LH, and HH coefficients. All the coefficients are discarded, except the LL coefficients that are transformed into the second level. The coefficients are then passed through a constant scaling factor to achieve the desired compression ratio. An illustration is shown in Fig. 2. Here, x[n] is the input signal, d[n] is the high frequency component, and a[n] is the low frequency component. For data reconstruction, the coefficients are rescaled and padded with zeros, and passed through the wavelet filters. We have used the Daubechies filter coefficient [29] in this work.

IV. Proposed Hybrid DWT- DCT Algorithm

The main objective of the presented hybrid DWT-DCT algorithm is to exploit the properties of both the DWT and the DCT. Giving consideration of the type of application, original image/frame of size *256×256* (or any resolution, provided divisible by 32) is first divided into blocks of *N×N*. Each block is then decomposed using the 2-D DWT. Low-frequency coefficients (LL) are passed to the next stage where the high-frequency coefficients (HL, LH, and HH) are discarded.

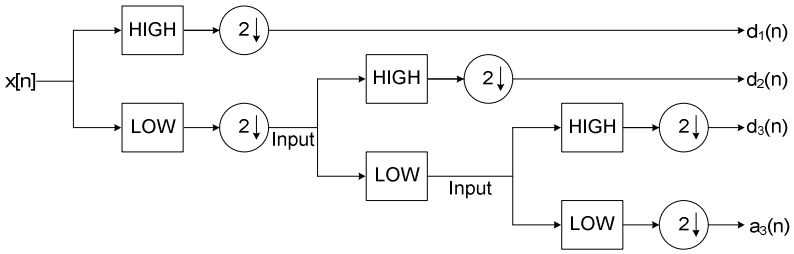

Fig. 2. Block diagram of the 2-level DWT scheme

The passed LL components are further decomposed using another 2-D DWT. The 8-point DCT is applied to these DWT coefficients. By discarding the majority of the high coefficients, we can achieve a high compression. To achieve further compression, a JPEG-like quantization is performed. In this stage, many of the higher frequency components are rounded to zero. The quantized coefficients are further scaled using scalar quantity known as scaling factor (SF). Finally, the image is reconstructed following the inverse procedure. During the inverse DWT, zero values are padded in place of the detail coefficients. The entire procedure is summarized below and illustrated in Fig. 3 (for *N*=32). The sub-sampling schemes used in this work are shown in Fig. 4.

A. Hybrid algorithm

The hybrid is briefly presented below:

SF = Scaling factor
SF_{old} = Starting Scaling Factor
ΔSF = increment of SF
$CR_{desired}$ = Maximum CR desired
M= Input data of dimension ($N \times N$)
W_{coeff} = wavelet filter coefficient
W_{wv} = 2D DWT coefficient
W_{iwv} = 2D IDWT coefficient
Z_{dct} = 2D DCT coefficient
Z_{idct} = 2D IDCT coefficient
Q = Q table
Z_{QN} = Quantized DCT coefficients
Z_{DQN} = De-quantized DCT coefficients
Z_{SF} = Scaled DCT coefficients
Z_{RSF} = Rescaled DCT coefficients

A.1 Compression Procedure

1. Compute 2-level 2D DWT coefficients of the input samples (N x N): $W_{w,v} = W_{coeff} \times M \times W'_{coeff}$

2. Perform 2D DCT on the four $W_{w/4,v/4}$ coefficients $\frac{N}{4} \times \frac{N}{4}$:

$$Z_{dct}(i,j) = \frac{1}{\sqrt{2N}} B(i) B(j) \sum\sum W_{w/4,v/4}(x,y) \times \cos\left[\frac{2x+1}{2N} i\pi\right] \times \cos\left[\frac{2y+1}{2N} j\pi\right]$$

for $i, j = 0, \ldots, \frac{N}{4} - 1$, $B(u) = \begin{cases} \frac{1}{\sqrt{2}} & if \quad u = 0 \\ 1 & if \quad u > 0 \end{cases}$

3. Quantize the four DCT coefficient matrices ($\frac{N}{4} \times \frac{N}{4}$) using four different Q tables:

$$Z_{QN}(i,j) = round\left(\frac{Z_{dct}(i,j)}{Q(i,j)}\right) \text{ for } i, j = 0, \ldots, \frac{N}{4} - 1$$

4. Calculate Compression ratio (CR):

If CR = $CR_{desired}$
Go to step 8 (End)
Else
Continue to step 5

5. Perform Scaling on the quantized coefficients, $Z_{QN}(i,j)$:

$$Z_{SF}(i,j) = round\left(\frac{Z_{QN}(i,j)}{SF_{old}}\right) \text{ for } i, j = 0, \ldots, \frac{N}{4} - 1$$

$SF_{old} = SF_{old} + \Delta SF$
$SF = SF_{old}$

6. Sub-sample the three higher order coefficient matrices, LH, HL, and HH (if needed)

7. Go to step 4

8. End

A.2 Reconstruction Procedure

1. Interpolate the three higher order coefficient matrices (zero padding)
2. Perform Rescaling
3. Perform De-Quantization
4. Compute 2D IDCT of the $\frac{N}{4} \times \frac{N}{4}$ samples
5. Compute 2-level 2D IDWT to get back the N x N reconstructed matrix
6. Calculate PSNR
7. Calculate SSIM
8. End

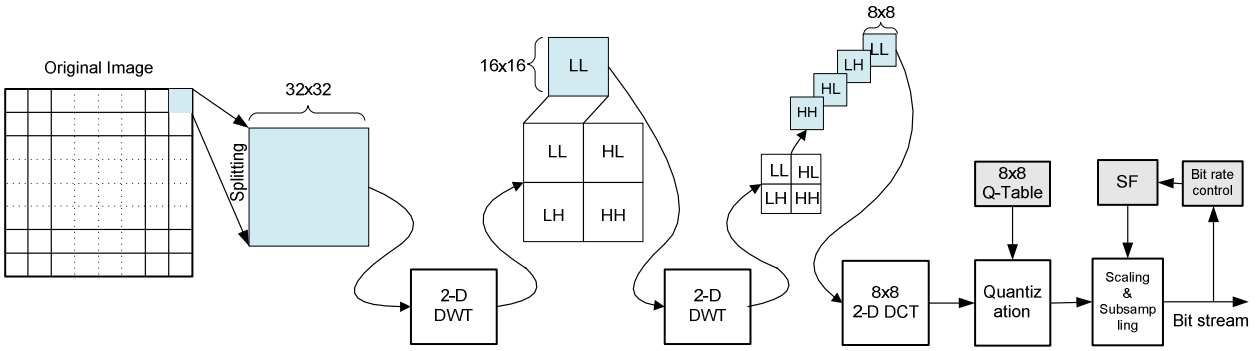

(a)

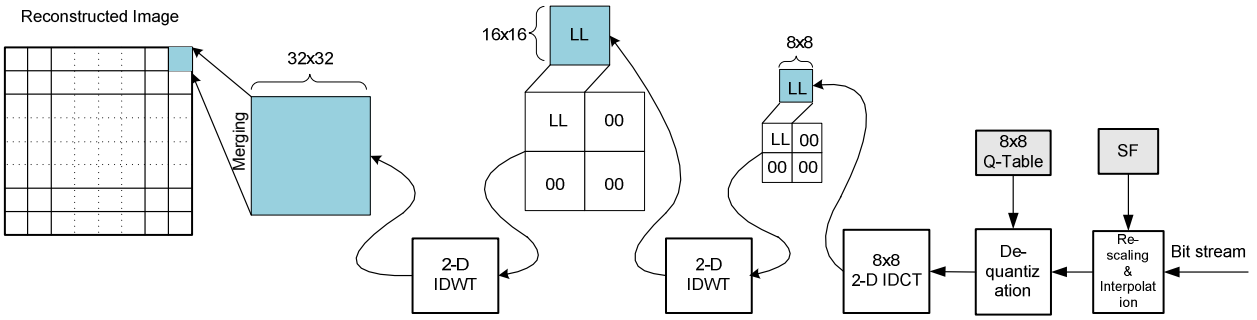

(b)

Fig. 3. Block diagram of the proposed hybrid DWT-DCT scheme for N=32: (a) compression algorithm; (b) decompression algorithm

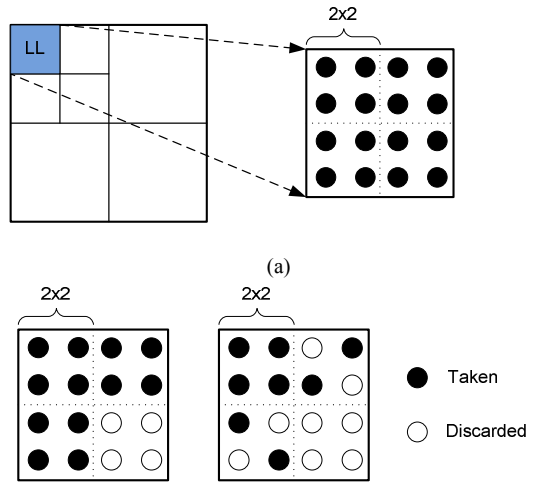

Fig. 4. Sub-sampling of the DWT coefficients: (a) fully sampled for LL; (b) quarterly sampled and half sampled for LH, HL, and HH

V. Evaluation Criterion

In this section, the performance of the algorithms using two popular measures: compression ratio (CR) and peak signal to noise ratio (PSNR) has been analyzed. Image having same PSNR value may have different perceptual quality. The Structural Similarity Metric (SSIM) index is another measurement technique that is proven to be well matched to perceived visual quality of the image [30]. By adjusting the parameters, trade-off can be achieved for compressed image against reconstructed image quality over wide a range.

A. PSNR

The PSNR in decibel is evaluated as follows:

$$PSNR = 10\log_{10}\frac{I^2}{MSE} \tag{3}$$

where, I is the maximum intensity level (= 255).

$$MSE = \frac{1}{MN}\sum_{i=1}^{M}\sum_{j=1}^{N}\left(A_{i,j} - B_{i,j}\right)^2 \tag{4}$$

where, A is the original image and B is the reconstructed image of size $M \times N$.

B. Compression ratio (CR)

The compression ratio is defined as follows:

$$CR = \frac{Discarded\ \ data}{Original\ \ data} \tag{5}$$

The resulting CR can be varied according to the image quality and the level of compression depends on the QT and the SF.

C. SSIM index

The SSIM index is the objective image quality measure and can be defined as below:

$$SSIM(A,B) = \frac{(2\mu_A\mu_B + C_1)(2\sigma_{AB} + C_2)}{(\mu_A^2 + \mu_B^2 + C_1)(\sigma_A^2 + \sigma_B^2 + C_2)} \quad (6)$$

Where, μ_A, μ_B = mean intensities of original data A and reconstructed data B; σ_A, σ_B = standard deviation of original data A and reconstructed data B; C_1, C_2 = constant.

$$\sigma_{AB} = \frac{1}{N-1}\sum_{i=1}^{N}(A_i - \mu_A)(B_i - \mu_B) \quad (7)$$

If the reconstructed data is retrieved exactly similar to original data then the best SSIM index of value 1 can be achieved.

VI. Performance Assessment

In order to evaluate the performance of the proposed hybrid algorithm, the algorithm has been applied to several images including medical images, benchmark images, and natural images. The reconstructions of the images are also reported. The natural images are captured by a Nikon D40X Digital Single Lens Reflex (DSLR) camera in raw format. The medical images include endoscopic images of different parts of Gastro Intestinal (GI) tract and some x-ray images. The types of images are categorized in TABLE I. All these sample images are shown in the Appendix.

TABLE I.
Types of image and video used for study

Image type		Video type
Type 1	Natural images [captured by Nikon D40X]	Endoscopic video [31]
Type 2	Medical images [32]	
Type 3	Bench mark images	

Furthermore, the algorithm is also applied on several endoscopic video sequences. The endoscopic videos show various parts of the intestine. Finally, the proposed algorithm has been verified using a Markov sequence.

A. Performance evaluation: Images

In this section, the performance evaluation parameters for images tabulated in TABLE I are presented. Fig. 5 shows the PSNR values obtained for the natural images at a constant CR of 96 % in case of DCT, DWT and proposed algorithm. In case of FWHT, the resulting PSNR value is very low (in the range of 7~15 dB) and the image reconstruction looks worst visually at higher CR as 96 %. Hence, it is compared at 87 % of CR. It is clear that, the proposed hybrid algorithm has higher PSNR compared to DCT, DWT, and FWHT algorithms. It is also clearly observed that FWHT has the least PSNR (less than 20 dB in average) even though it is compared only at CR of 87 %. The image number 3, 6, 8, and 10 are gradient images and they consist of dark colours such as red, green, and black. It is observed that for these images, the hybrid algorithm has the highest *PSNR* and outperforms the other three algorithms by a good margin.

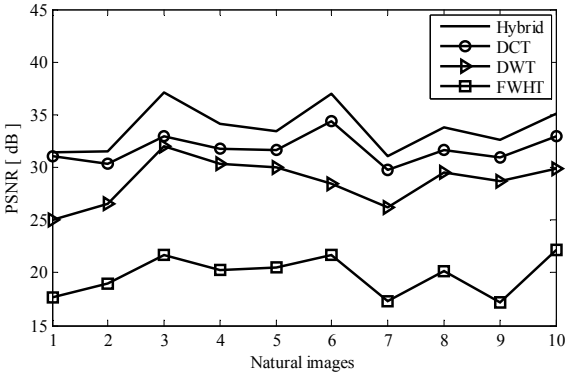

Fig. 5. PSNR for type 1 images for average CR of 96%

The typical value for image compression ranges from 20 ~ 40 dB [7-8]. The compression ratio comparison at the constant PSNR should lie within the above range. Since the PSNR value for the FWHT is less than 20 dB in average at 87% of compression ratio, it is not considered for the compression ratio comparison studies for all types of images and endoscopic videos presented in this work.

Since this research work is based on high compression ratio, the next algorithm having least PSNR is DWT algorithm. The average PSNR for the DWT is around 28dB. In order to achieve same PSNR for the proposed and DCT algorithms, the CR of these two algorithms has to be decreased. Fig. 6 shows the CR of different algorithm for a fixed PSNR for 28dB. It can be seen that the CR obtained by proposed algorithm is higher compared to other algorithms. In case of the DWT, since the compression depends only on the number of level of decomposition, the CR stays as constant in Fig. 6.

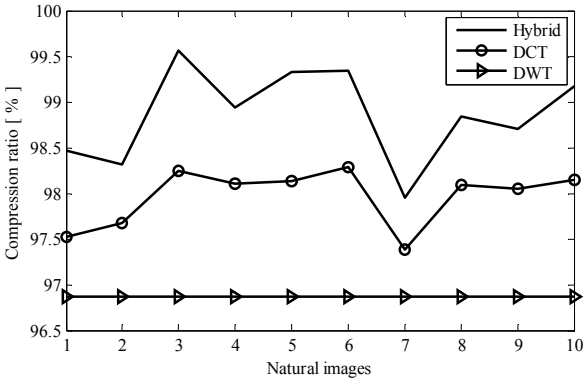

Fig. 6. CR for type 1 images for average PSNR of 28 dB

Similarly, the SSIM index for type 1 images are calculated for DCT, DWT and proposed algorithm at CR of 96 % and for FWHT algorithm at 87 % and plotted in Fig. 7. It is observed that for this constant CR, the SSIM index is higher for the hybrid DWT-DCT scheme.

The original and reconstructed images for one of the type 1 images are shown in Fig. 8. The PSNR values for reconstructed image using, DCT, DWT, FWHT, and hybrid algorithm are 31dB, 25dB, 23.48dB, and 31.8dB respectively. The FWHT has very low PSNR as compared to other algorithms in this case, and hence the reconstruction quality is least. Therefore, visual illustration of the reconstruction quality of the FWHT has been discarded for all types of images and videos in this work. The false contouring effect is clearly visible in the image reconstructed by the DCT and it is due to the high compression ratio. However, the reconstructed image obtained using proposed algorithm is free from contouring effect even though the PSNR difference between DCT and proposed algorithm is only 0.8dB.

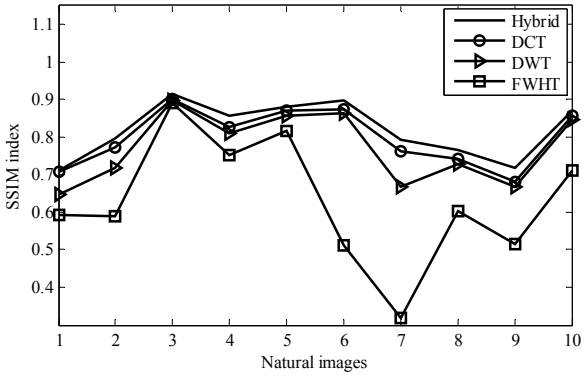

Fig. 6. SSIM index for type 1 images for average CR of 96%

Next, we present the results for type 2 medical images. In Fig. 9, we present the comparison results for sixteen medical images at constant compression ratio of 96%. Previous research on image compression suggests the acceptable PSNR for medical images should be equal or greater than 35 dB [9-10]. It is observed from Fig. 9, that, even for very high CR of 96%, the PSNR value for the proposed algorithm is higher than 35dB – this satisfies the acceptability of the proposed scheme for the compression of medical images. It is also observed that for specific compression ratio, PSNR using proposed hybrid algorithm outperforms the other three algorithms. In this case, since the average PSNR for the DWT is around 32 dB, the CR is performed at that particular PSNR of 32 dB. The resulting plot is shown in Fig. 10.

Fig. 11 shows the comparison plots of SSIM index of the medical images for constant CR of 96% for DCT, DWT and proposed algorithm. It is observed that the value of SSIM index using the proposed hybrid algorithm is the highest and the range of SSIM index for endoscopic image is from 0.45 – 0.85, whereas for X-ray images, the value of SSIM index is between 0.75-0.95. The original and reconstructed images for one of the type 2 images are shown in Fig. 12.

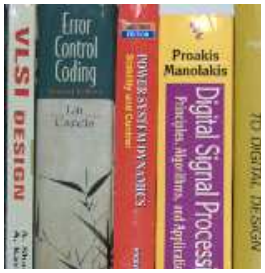

(a) Original image

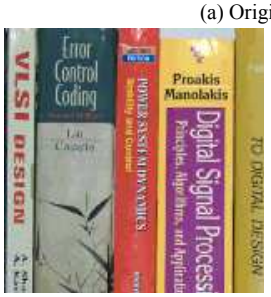

(b) PSNR = 31 dB

(c) PSNR = 25 dB

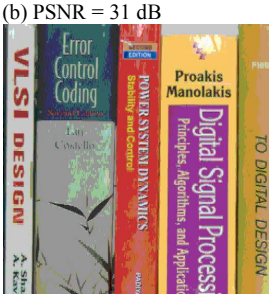

(d) PSNR= 23.48 dB

(e) PSNR= 31.8 dB

Fig. 7. (a) Original, and reconstructed natural image using (b) DCT, (c) DWT, (d) FWHT, (e) Hybrid

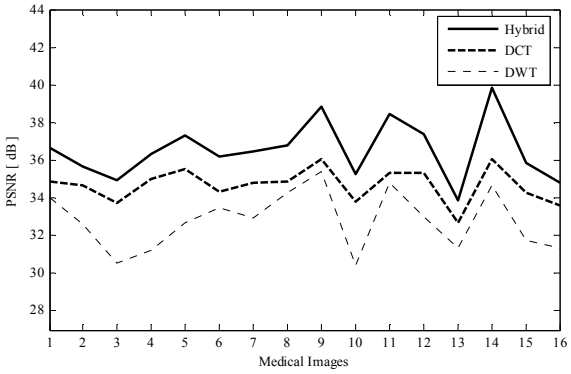

Fig. 8. PSNR for type 2 images for average CR of 96%

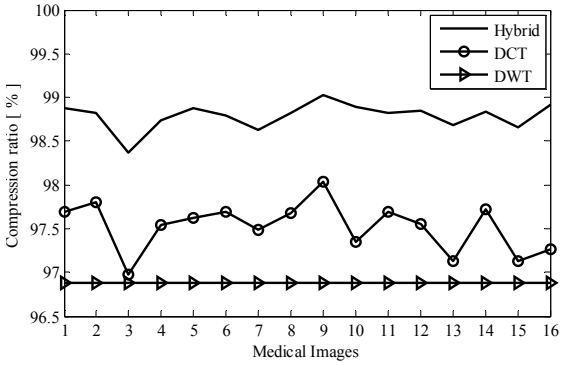

Fig. 9.CR for type 2 images for average PSNR of 32 dB

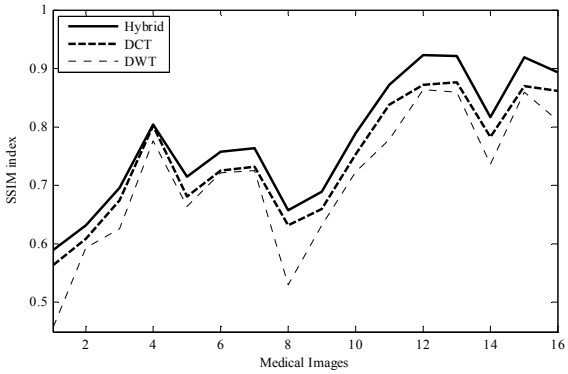

Fig. 10. SSIM index for type 2 images for average CR of 96%

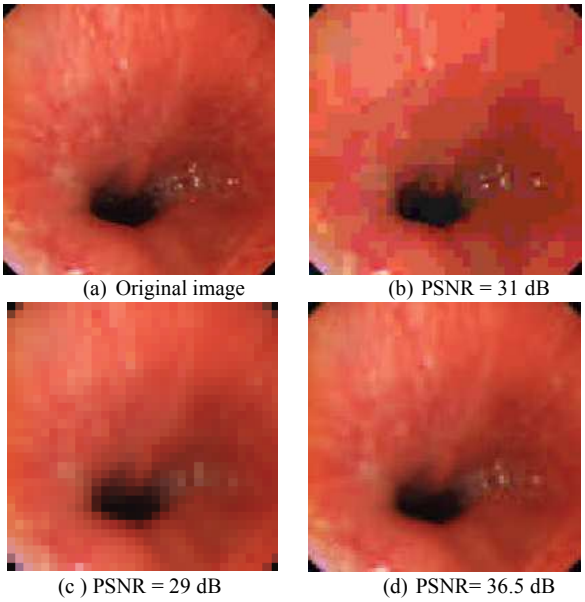

(a) Original image (b) PSNR = 31 dB

(c) PSNR = 29 dB (d) PSNR= 36.5 dB

Fig. 11. (a) Original, and reconstructed medical image using (b) DCT, (c) DWT, (d) Hybrid

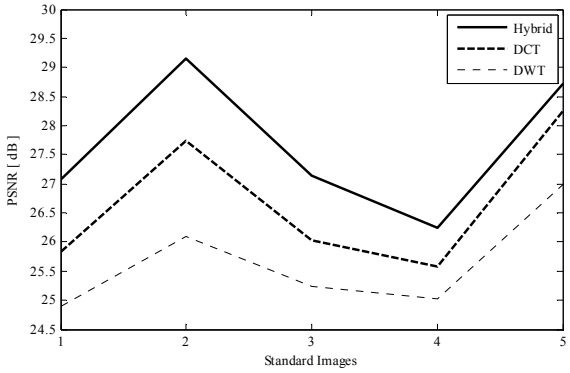

Fig. 12. PSNR for type 3 images for CR of 96%

The proposed hybrid algorithm is tested on some benchmark (standard) images. Fig. 12 shows the plot of PSNR for five different types of benchmark images for a constant CR of 96% for DCT, DWT and proposed algorithm. Fig. 13 shows the plot of CR for the average PSNR of 25dB. The SSIM index for the benchmark images is illustrated in **Error! Reference source not found.**. Like the other two image types, the hybrid scheme performs much better than the other three schemes in all cases. Fig. 16 shows the reconstructed images. Like the previous case, the false contouring effect is visible in the image reconstructed by the DCT. The image reconstructed by the DWT is also very poor compared to the one with the proposed hybrid algorithm.

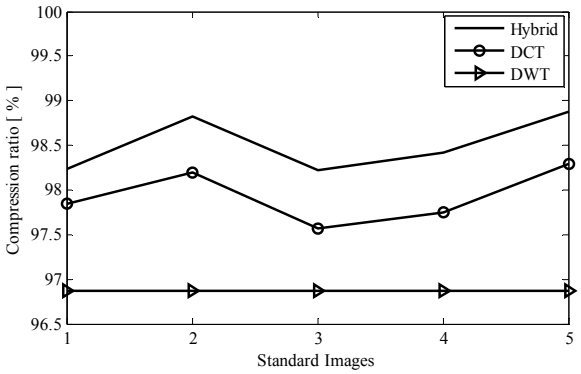

Fig. 13. CR for type 3 images for average PSNR of 25 dB

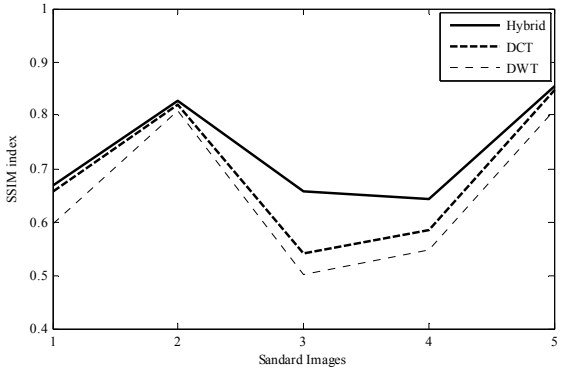

Fig. 14. SSIM index for type 3 images for average CR of 96%

B. Performance evaluation: Endoscopic video

In order to show the performance advantage in video signals, we have applied the hybrid DWT-DCT algorithm to several Endoscopic video clips. Note that, the proposed algorithm has been applied to spatial domain only, i.e., the video is treated as series of still frames. It is observed that performance of the FWHT algorithm is least as compared to other standalone DCT and DWT and proposed algorithm and the PSNR value is less than 20 dB in average for all types of images for 87% compression ratio, hence in this section, the performance of the FWHT algorithm is not considered for the analysis.

Fig. 17 reveals the PSNR all three algorithms for the first 30 frames of five endoscopic videos at a compression ratio, 98%. It can be seen that at such high CR, the PSNR achieved by the hybrid and the DCT algorithm are very close. As described earlier, the DWT has a constant CR due to constant level of decomposition. Fig. 18 shows the CR for a constant PSNR of 23.5dB. In Fig. 19, we present the first frame of one endoscopic video along with other reconstructed frames using three schemes. The false contouring effect due to extreme compression (i.e., 98%) is clearly visible in the frame reconstructed using the JPEG-based DCT.

(a) Original image

(b) PSNR = 25.98 dB

(c) PSNR = 23.42 dB

(d) PSNR= 22.37 dB

(e) PSNR= 30.41 dB

Fig. 15. (a) Original, and reconstructed benchmark image using (b) DCT, (c) DWT, (d) FWHT,(e) Hybrid

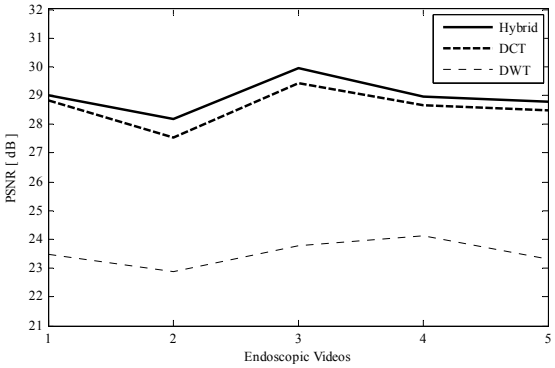

Fig. 17. Average PSNR for type 1 videos for average CR of 98%

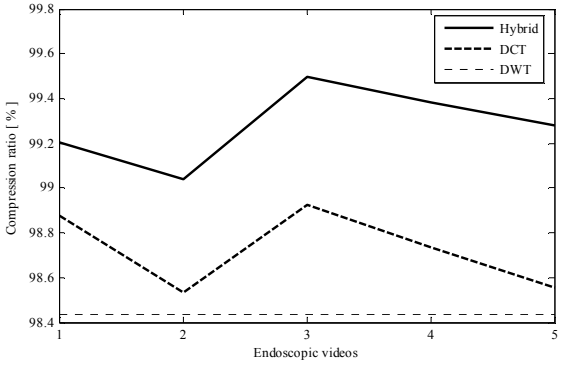

Fig. 18. Average compression ratio for type 1 video for average PSNR of 23.5 dB

(a) Original frame

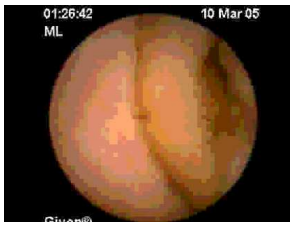

(b) PSNR = 27.94 dB

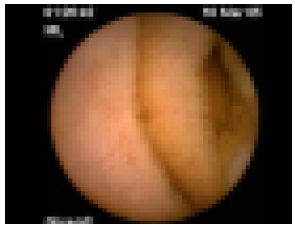

(c) PSNR = 23.49 dB

(d) PSNR= 28.98 dB

Fig. 19. (a) Original, and reconstructed frame of type 1 video using (b) DCT, (c) DWT, (d) Hybrid

C. Distribution of Variance

The algorithm is tested for first order Markov sequence having the correlation matrix of size $N = 16$ and correlation coefficient, $\rho = 0.95$. The correlation matrix is given below in Eq. (8) [11]. The variances, σ_k^2, are represented by the *Eigen* values of the transformed coefficient. All the three algorithms are analyzed to compute the rate distortion. Fig 20 shows the distribution of variances of the transform coefficients (in decreasing order) for three different transforms.

$$R = \begin{bmatrix} 1 & \rho & \rho^2 & . & . & . & \rho^{N-1} \\ \rho & 1 & . & . & . & . & . \\ . & . & . & . & . & . & . \\ . & . & . & . & . & . & . \\ . & . & . & . & . & . & \rho^2 \\ . & . & . & . & . & . & \rho \\ \rho^{N-1} & . & . & . & . & \rho & 1 \end{bmatrix} \qquad (8)$$

Fig 20 shows the distribution of variances of the transform coefficients (in decreasing order) for three different transforms. In this plot, the CR for the DCT, the DWT and the hybrid schemes have been set to 50%, 53% and 50% respectively. It can be seen that, for a given CR, the hybrid scheme has the lowest variance distribution, which leads to higher PSNR compared to the other two schemes, as evident in other plots. In other words, for a fixed level of distortion, the number of bits required to transmit the hybrid transformed coefficients would be less than those required for other schemes.

D. Performance assessment with noise

Here, the proposed algorithm is tested under a noisy environment. The Gaussian white noise is added to the image ("lena" and medical image) and the performance of the proposed algorithm is compared with the DCT and the DWT.

The results are tabulated in the TABLE II. It shows that proposed algorithm performs better than other schemes.

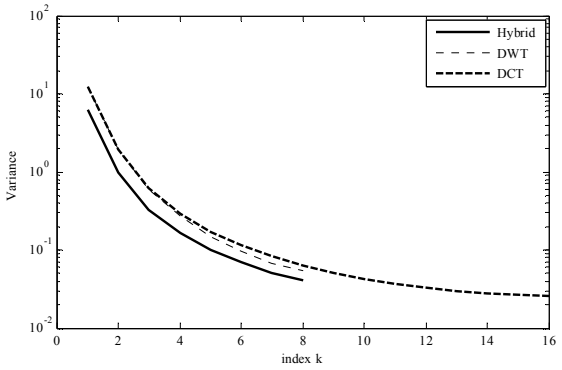

Fig. 20. Variance distribution of the transform coefficients

TABLE II.
PERFORMANCE OF ALGORITHMS AFTER ADDING GAUSSIAN NOISE

Variance	Image	PSNR (dB)		
		DCT	DWT	Hybrid
0.001	Lena	21.1	19.7	**21.1**
	Medical	29.4	28.4	**29.7**
0.004	Lena	23.4	21.5	**23.4**
	Medical	23.7	23.6	**24.3**
0.008	Lena	26.3	23.8	**27.0**
	Medical	21.2	20.8	**21.5**

E. Comparisons with other hybrid schemes

In order to show the effectiveness of the proposed hybrid DWT-DCT scheme, the algorithm has been compared with some standards: JPEG, JPEG2000, and existing hybrid algorithms. TABLE III shows the comparison results using standard images: Lena, Barbara and Goldhill. From the table, it is clearly observed that for the standard images, the proposed hybrid algorithm performance is better than the performance of other standard schemes and hybrid algorithms.

TABLE III. RESULT COMPARISON WITH OTHER ALGORITHMS

Test images		PSNR (dB)		
		Lena	Barbara	Goldhill
CR = 32 % (bpp = 0.25)	HS-HIC [15]	35.0	26.1	30.5
	Yu & Mitra [17]	35.0	31.5	32.9
	JPEG	32.4	27.7	29.7
	JPEG2000	34.1	28.8	30.5
	OB-HIC [16]	35.9	32.8	33.8
	Proposed	**36.9**	**31.4**	**35.8**

In addition, the proposed algorithm is also compared with [12] using various medical images: CT, US, and X-ray images. The proposed algorithm is compared with [12] at various compression level as shown in TABLE IV. It is observed from the table that for all medical images, the gain in PSNR using the proposed hybrid algorithm is better than the method proposed in [12]. The reconstructed images are shown in Fig. 21 and 22. The SSIM index is given in Table V.

TABLE IV. RESULT COMPARISON WITH SING ET AL. [12]

Image types	bpp	PSNR (dB)	
		Singh et al. [12]	Proposed
CT images	0.234	34.6	**35.6**
	0.254	34.0	**55.9**
	0.273	32.5	**42.1**
	0.306	32.2	**44.0**
	0.356	31.1	**32.8**
US images	0.179	31.2	**31.3**
	0.204	31.4	**32.7**
	0.24	31.0	**36.5**
	0.312	30.3	**32.6**
	0.482	28.1	**29.7**
X-ray images	0.174	35.0	**44.7**
	0.187	34.9	**36.0**
	0.204	37.1	**40.7**
	0.225	34.4	**57.8**
	0.245	33.2	**47.6**

TABLE V.
SSIM MEASUREMENT

Image	SSIM index		
	DCT	DWT	Hybrid
CT	0.8681	0.8084	**0.9283**
US	0.8446	0.7411	**0.8976**

The computational complexity is given in Table VI. The proposed hybrid scheme has lesser complexity than the DCT, but higher than the DWT.

TABLE VI.
COMPUTATIONAL COMPLEXITY

Scheme	Unit complexity	Total complexity (for 32 x 32 block)
DCT	$O(N \log_2 N)$	$O((8\log_2 8)\times 16)$
DWT	$O(N)$ for 1-level	$O(32)+O(16)$
Hybrid	$O(\frac{N}{4}\log_2 \frac{N}{4})+O(N)$	$O(8\log_2 8)+O(32)+O(16)$

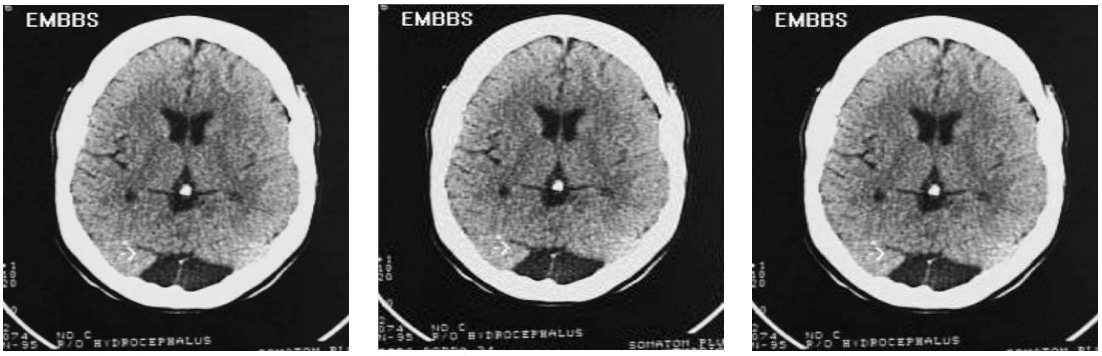

(a) original CT image (b) 31.13dB (c) 32.83dB

Fig. 21. Quality comparison at CR of 22.47% (a) Original image, (b) Singh et al. [12] (c) Proposed algorithm

(a) original US image (b) 28.12dB (c) 29.76dB

Fig. 22. Quality comparison at CR of 16.59% (a) Original image, (b) Singh et al.[12] (c) Proposed algorithm

VII. Conclusion

In this paper, we present a new hybrid scheme combing the DWT and the DCT algorithms under high compression ratio constraint. The algorithm performs the DCT on the lowest level DWT coefficient. It is tested on several types of images, such as, natural, medical, endoscopic, etc., as well as several endoscopic videos. The results of this exhaustive simulation show consistent improved performance for the hybrid scheme compared to the JPEG-based DCT, the Daubechies-based DWT, and the FWHT schemes. The new scheme performs better in a noisy environment and reduces the false contouring effects and blocking artifacts significantly. The analysis shows that for a fixed level of distortion, the number of bits required to transmit the hybrid coefficients would be less than those required for other schemes. The proposed scheme has medium computational complexity and is intended to be used as the image/video compressor engine in imaging and video applications.

References

[1] R. K. Rao and P. Yip, Discrete Cosine Transform: Algorithms, Advantages and Applications. NY: Academic, 1990.

[2] W. B. Pennebaker and J. L. Mitchell, JPEG Still Image Data Compression Standard, 3rd ed. New York: Springer, 1993.G. O. Young, "Synthetic structure of industrial plastics (Book style with paper title and editor)," in *Plastics*, 2nd ed. vol. 3, J. Peters, Ed. New York: McGraw-Hill, 1964, pp. 15–64.

[3] G. Joy and Z. Xiang, "Reducing false contours in quantized color images," Computer and Graphics, Elsevier, vol. 20, no. 2, pp. 231–242, 1996.

[4] L. Chen, VLSI Design of Wavelet Transform: Analysis, Architecture and Design Examples. Imp. College press, 2007.

[5] R. A. DeVore, B. Jawerth, and B. J. Lucier, "Image compression through wavelet transform coding," IEEE Transactions on Information Theory, vol. 38, no. 2, pp. 719–746, 1992.

[6] G. Strang and T. Nguyen, Wavelets and Filter Banks. Cambridge Press, 1996.

[7] N. Thomos, N. V. Boulgouris, and M. G. Strintzis, "Optimized transmission of JPEG2000 streams over wireless channels," IEEE Transactions on Image Processing, vol. 15, no. 1, pp. 54–67, 2006.

[8] X. Li and J. Cai, "Robust transmission of JPEG2000 encoded images over packet loss channels," in Proc. IEEE Int Multimedia and Expo Conf, 2007, pp. 947–950.

[9] H. N. K. A. Saffor, A. R. Ramil and D. Dowsett, "Objective and subjective evaluation of compressed computed tomography images," Internet Journal of Radiology, vol. 2, no. 2, 2002.

[10] S. Garawi, R. S. H. Istepanian, and M. A. Abu-Rgheff, "3 G wireless communications for mobile robotic tele-ultrasonography systems," IEEE Communications Magazine, vol. 44, no. 4, pp. 91–96, 2006.

[11] A. K. Jain, Fundamentals of Digital Image Processing. Prentice Hall Inc., 1989.

[12] S. Singh, V. Kumar, and H. K. Verma, "DWT-DCT hybrid scheme for medical image compression." J Med Eng Technol, vol. 31, no. 2, pp. 109–122, 2007.

[13] Suchitra Shrestha and Khan Wahid, "Hybrid DWT-DCT Algorithm for Biomedical Image and Video Compression Applications", Proc. of the 10th IEEE International Conference on Information Sciences, Signal Processing and their Applications, pp. 280-283, 2010.

[14] M. Ezhilarasan and P. Thambidurai, "A hybrid transform technique for video coding," LNCS, vol. 4308, pp. 503–508, 2006.

[15] U. S. Mohammed, "Highly scalable hybrid image coding scheme," Digital Signal Processing,Science Direct, vol. 18, pp. 364–374, 2008.

[16] U. S. Mohammed and W. M. Abd-elhafiez, "Image coding scheme based on object extraction and hybrid transformation technique," Int. J. of Engineering Science and Technology, vol. 2, no. 5, pp. 1375–1383, 2010.

[17] T.-H. Yu and S. K. Mitra, "Wavelet based hybrid image coding scheme," in Proc. IEEE Int Circuits and Systems Symp, vol. 1, 1997, pp. 377–380.

[18] R. Singh, V. Kumar, and H. K. Verma, "DWT-DCT hybrid scheme for medical image compression," Medical Engineering and Technology, vol. 31, pp. 109–122, 2007.
[19] F. Zhijun, Z. Yuanhua, and Z. Daowen, "A scalable video coding algorithm based DCT-DWT," in Proc. 3rd IEEE Int. Symp. Signal Processing and Information Technology, 2003, pp. 247–249.
[20] P. J. Paul and P. N. Girija, "A novel VLSI architecture for image compression," in Proc. ISM'06 Multimedia Eighth IEEE Int. Symp, 2006, pp. 794–795.
[21] [21] K. A. Wahid, M. A. Islam, S. S. Shimu, M. H. Lee, and S. Ko, "Hybrid architecture and VLSI implementation of the Cosine-Fourier-Haar transforms," Circuits, Systems, and Signal Processing, vol. 29, no. 6, pp. 1193–1205, 2010.
[22] S. Jiang and X. Hao, "Hybrid Fourier-Wavelet image denoising," Electronics Letters, vol. 43, no. 20, pp. 1081–1082, 2007.
[23] A. H. Ali, "Combined DWT-DCT digital image water marking," Computer science, vol. 3, no. 9, pp. 740–746, 2007.
[24] H. Qi, Q. Huang, and W. Gao, "A low-cost very large scale integration architecture for multistandard inverse transform," IEEE Transactions on Circuits and Systems II: Express Briefs, vol. 57, no. 7, pp. 551–555, 2010.
[25] C. Fan and G. Su, "Fast algorithm and low-cost hardware-sharing design of multiple integer transforms for VC-1," IEEE Transactions on Circuits and Systems II: Express Briefs, vol. 56, no. 10, pp. 788–792, 2009.
[26] C. P. Fan and G. A. Su, "Efficient fast 1-d 8 × 8 inverse integer transform for VC-1 application," IEEE Transactions on Circuits and Systems for Video Technology, vol. 19, no. 4, pp. 1–7, 2009.
[27] K. Wahid, S.-B. Ko, and D. Teng, "Efficient hardware implementation of an image compressor for wireless capsule endoscopy applications," in Proc. IEEE Int. Joint Conf. Neural Networks, 2008, pp. 2761–2765.
[28] J. D. Kornblum, "Using JPEG quantization tables to identify imagery processed by software," Digital Forensic Workshop, Elsevier, pp. 21–25, 2008.
[29] I. Daubechies, Ten Lectures on Wavelets. SIAM, 1992.
[30] H. S. Z. Wang, A. Bovik and E. Simoncelli, "Image quality assessment: From error measurement to structural similarity," IEEE Trans. Image Processing, vol. 13, no. 4, pp. 600–612, 2004.
[31] D. O. Faigel and D. R. Cave, Capsule endoscopy. Elsivier, 2008.
[32] "Gastrolab-the gastrointestinal site," Aug 28 2010. [Online]. Available: www.gastrolab.net W.-K. Chen, *Linear Networks and Systems* (Book style). Belmont, CA: Wadsworth, 1993, pp. 123–135.

APPENDIX: SAMPLE IMAGES USED FOR PERFORMANCE ANALYSIS

Type 1 Images: Natural images

Type 2 Images: Medical images

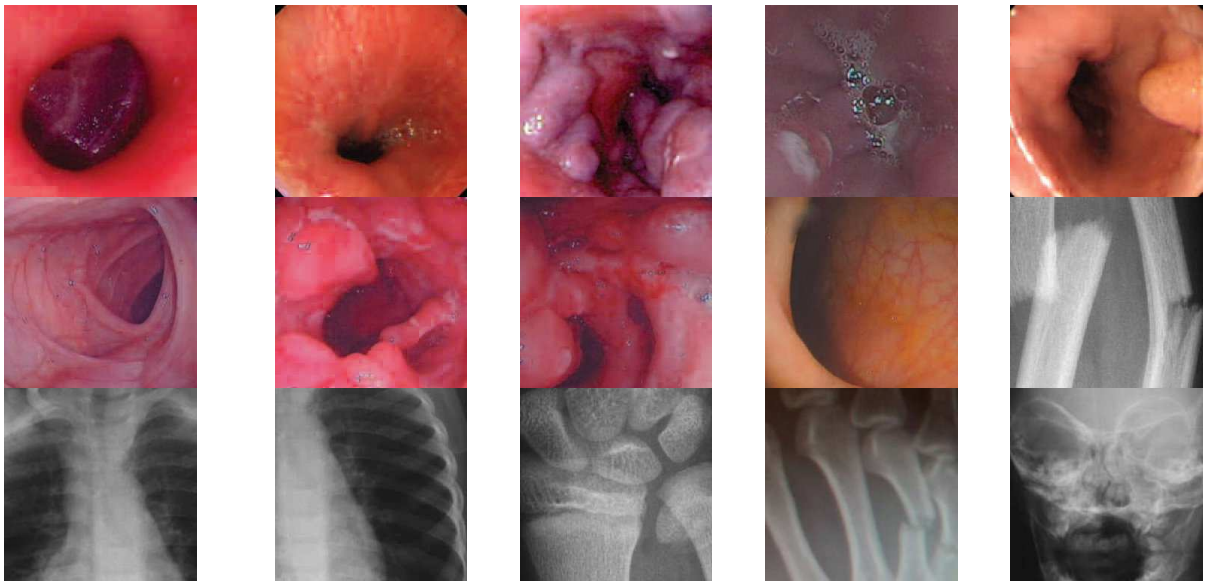

Type 3 Images: Benchmark images





Suchitra Shrestha received the Bachelor's degree (B.E.) in Electrical Engineering from Tribhuvan University (T.U.), Nepal in 2004. She obtained M.Sc. degree in Telecommunication Engineering from the Inha University, South Korea in 2008. She is currently M. Sc. student in University of Saskatchewan, Saskatoon, Canada. Her research interest includes Image compression system, Digital Signal processing.

Khan Wahid earned his B.Sc. degree from Bangladesh University of Engineering and Technology (BUET) in 2000. He received his M.Sc. (2003) and Ph.D. (2007) from the University of Calgary. He was the recipient of numerous prestigious awards and scholarships including the most distinguished "Killam Scholarship" and the "NSERC Canada Graduate Scholarship" for his doctoral research.

Dr. Wahid has been working as an Assistant Professor in the Department of Electrical and Computer Engineering at the University of Saskatchewan since July 2007. He has authored (and co-authored) over 40 peer-reviewed journal and international conference papers in the field of digital arithmetic techniques, FPGA and ASIC design, real-time embedded systems, video and image compression, and biomedical imaging systems. He has been serving as a reviewer for the IEEE Transactions on Circuit and Systems for Video Technology, Biomedical Engineering Online, EURASIP Journal on Signal Processing, and Elsevier Journal on Computers and Electrical Engineering since 2006. He is currently a registered Professional Engineer in the province of Saskatchewan, Canada and a Member of the Institute of Electrical and Electronics Engineers (IEEE).